COMPARATIVE STUDY OF DYNAMIC BEHAVIOUR OF PMSM DRIVE USING LINEAR QUADRATIC REGULATOR (LQR) BASED STATE FEEDBACK CONTROL (SFC) WITH DIFFERENT INTEGRAL CONTROL ACTIONS

Pranjal Das – Soujanya Hazra – Akshat Thapa – Archak Sadhukhan – Prem Kumar Sarkar – Pritam Kumar Gayen*

Department of Electrical Engineering, Kalyani Government Engineering College, Kalyani, West Bengal, India

ARTICLE INFO

Article history:

Received: 07.11.2024.

Received in revised form: 08.02.2025.

Accepted: 12.02.2025.

Keywords:

Permanent Magnet Synchronous Motor State Feedback Control Linear Quadratic Regulator Integral Speed Error Dynamic Performance

DOI: https://doi.org/10.30765/er.2708

Abstract:

The goal of this work is to compare the dynamic performances of a permanent magnet synchronous motor (PMSM) drive under various speed conditions by using different integral control actions with a linear quadratic regulator (LQR) based state feedback control (SFC) technique. Here, the two types of integral actions on speed error are used in the models of LQR-SFC controllers (namely, LQR-SFC-PI and LQR-SFC-ISE). The relative dynamic performances for the two models of speed controllers are observed under the rise or fall of the machine's speed. In the conditions, the rise time and steady-state error are less in the case of the LQR-SFC-PI model, whereas peak overshoot or undershoot and settling time are less for the LQR-SFC-ISE model. At the starting moment, the LQR-SFC-PI model fails to achieve the desired speed for the large rise of speed, but the LQR-SFC-ISE model converges to the speed reference.

1 Introduction

The usage of permanent magnet synchronous machines [1] is increasing in different fields of electrical or electronics engineering, such as wind energy conversion systems, electric vehicles, robotics, machine tools etc. The advantages of the machine are high starting torque, good efficiency, high torque/weight ratio, etc [2]. In speed control applications such as electric vehicles, high dynamic performance of the permanent magnet synchronous motor (PMSM) drive [3] is an important requirement. In this regard, direct torque control and vector control techniques are noticed in practice. The literature suggests that the DTC method is a straightforward technique to implement as it does not involve a current control loop, but this method produces more torque ripples in the machine [4]. On the other hand, the vector control method provides decoupled control of torque and flux in the machine. But it involves three control loops (a speed control loop and two current control loops), which need special attention to tune different controllers. The appropriate tuning is not possible to get the optimum dynamic response of the machine's speed. Therefore, state feedback control (SFC) of PMSM [5] is necessary to achieve optimal speed control of the machine, and here, the high dynamic performance of the machine can be conveniently achieved. In some papers, the pole placement-based SFC [6] is applied to control PMSM to get a better dynamic response than the multi-loop vector control method. Here, the target pole location is difficult to decide.

Thus, the optimum dynamic performance of the pole placement method is a difficult task. In the advancement of control methods, the linear quadratic regulator (LQR)-based SFC method is used to avoid the choice of suitable poles. In this context, various LQR-SFC methods [7-11] are suggested to achieve the enhanced performances of the speed-regulating loop. The findings and shortcomings of these methods are discussed in subsection 1.1. Then, the research gap and contributions of the proposed work are mentioned in

E-mail address: pkgtar@gmail.com

^{*} Corresponding author

subsections 1.2 and 1.3, respectively. In this paper, two types of integral control action along with the standard LQR-SFC method are used for a PMSM drive to obtain improved dynamic performance. The responses under different speed conditions along with load torque variations are observed in two integral control actions, and the performance indexes of dynamic responses are compared. Therefore, the results of diversified tests reveal comparative views on the impacts on the speed control loop by the two techniques.

1.1 Literature Review

The LQR-SFC logics based on the linearised model of PMSM in the recent works are reviewed and listed in Table 1, which highlights the findings and shortcomings of the prior studies.

Prior works	Findings		Shortcomings
[5]	i. To improve disturbance rejection, a third- order augmented system is built,ii. Resilience to parametric change.		
[7]	i. Mitigation of periodic torque and speed variations,		TI I :
	ii. Restricts the external disturbance's noisy effects.	1.	The dynamic performance at the
[8]	The operational point of the suggested non- linear disturbance observer is adaptively updated.		starting moment is not investigated.
[9]	For sensor-less control, the sliding mode observer and disturbance observer are suggested.	ii.	The comparative study among different integral actions with LQR-SFC
[10]	A new state feedback control algorithm that incorporates current, current error, and current error integration is suggested.		model for dynamic speed variations of PMSM are not
[11]	When plant parameters change, the artificial bee colony optimization technique is utilized to modify the state-feedback speed controller's coefficients, paying special attention to the moment of inertia.		observed.

Table 1. Performances of state-of-arts.

1.2 Research Gap

The comparative study among different integral actions with LQR-SFC model for dynamic speed variations of PMSM are not observed in the above discussed recent studies. Also, the tracking of the speed variations at the starting moment using LQR-SFC method is not investigated.

1.3 Contributions

From the literature review and research gap, the contributions of the proposed works are mentioned as,

- i. The comparative performances of the different integral actions on speed error along with LQR-SFC control are investigated,
- ii. The settling to the reference speed after the speed variations at the starting moment is observed.

The fundamentals of PMSM drive are cited in Section 2. The conventional LQR-SFC technique is presented in Section 3. Section 4 discusses the different schemes of integral control action based LQR-SFC method. Section 5 provides the various tests, results, and comparative performances. Finally, Section 6 concludes and discusses the findings.

2 Fundamentals of PMSM drive

High-performance drives are characterized by their ability to offer precise control, rapid dynamic response, and good steady-state response [12]. Various control methods of AC motor are mentioned in Figure 1. Controlling the speed, flux, and torque of AC machines involves several techniques. The primary control parameters are the voltage and frequency of the applied voltages/currents [13]. In many cases, AC-DC-AC converters are used for AC machine drives due to their flexibility of power conversion. These converters are used for controlling AC motors in variable speed applications. Alternative options include direct AC-AC converters like cyclo-converters and matrix converters. However, these alternatives have certain drawbacks, such as the limited output frequency of cyclo-converters and the matrix converter's ability to achieve only 86% of the input voltage magnitudes. However, with the help of power converter, the development of vector control (VC) in the early 1970s revolutionized the control of AC motors, making it possible to adjust torque and flux of AC machine in decoupled manner similarly to separately excited DC motors, thereby enhancing the efficiency of AC drives [14]. The VC involves the regulation of the instantaneous positions of voltage, current, and flux space vectors, ensuring correct orientation of the controlled vector in both steady state and transient conditions. This method is applicable to both asynchronous and synchronous motor drives [4].

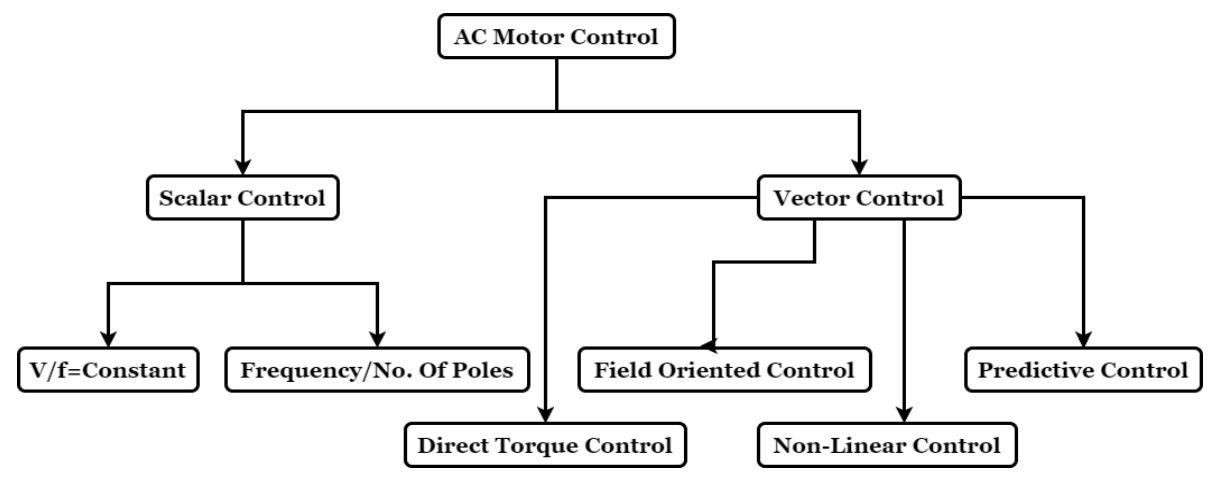


Figure 1. AC motor control schemes.

Vector control, also known as field-oriented control (FOC), involves managing the stator currents, which are represented as a vector [15]. This control technique uses matrix transformations to convert a three-phase balanced, time and speed dependent system into a two axis (d-q axis), time-invariant system. These technique gives the feasibility to control in two axis coordinate which leads to simplified control techniques. For speed control of PMSM using field-oriented control, requires two constant input reference signals - the component for torque (which is aligned with the q axis) and the flux component (which is aligned with the d axis) [16]. Since FOC relies solely on projections of vectors on the two-axis, it can manage instantaneous electrical quantities [17]. This attribute allows for precise control in all operating conditions (both steady state and transient). The motor three-phase currents are measured, Clarke and Park transformations convert the currents to the d-q reference frame, VC technique is performed [15], then inverse Clarke and Park transformations are applied to obtain the reference three-phase voltages which are used to calculate the gate pulses for the inverter and finally the motor is fed from the inverter. The multiloop control is used for the speed control of PMSM. It utilizes a two-loop structure: an outer loop for speed control and an inner loop for current control [15, 17]. The outer loop adjusts the reference current based on the speed error, and the inner loop ensures the motor currents follow this reference, achieving precise speed control.

The FOC architecture typically involves the following steps:

- i. Clarke and Park transformations: Convert the three-phase stator currents to the d-q frame using Clarke and Park transformations.
- ii. Current control loops: Use PI controllers to regulate the i_d and i_q currents.
- iii. Decoupling compensation: Compensate for the cross-coupling effects between d- and q-axis voltages.
- iv. Inverse Park and Clarke transformations: Convert the d-q voltages back to three-phase voltages for

PWM generation.

v. Speed control loop: An outer loop PI controller to regulate the rotor speed by providing the reference iq current.

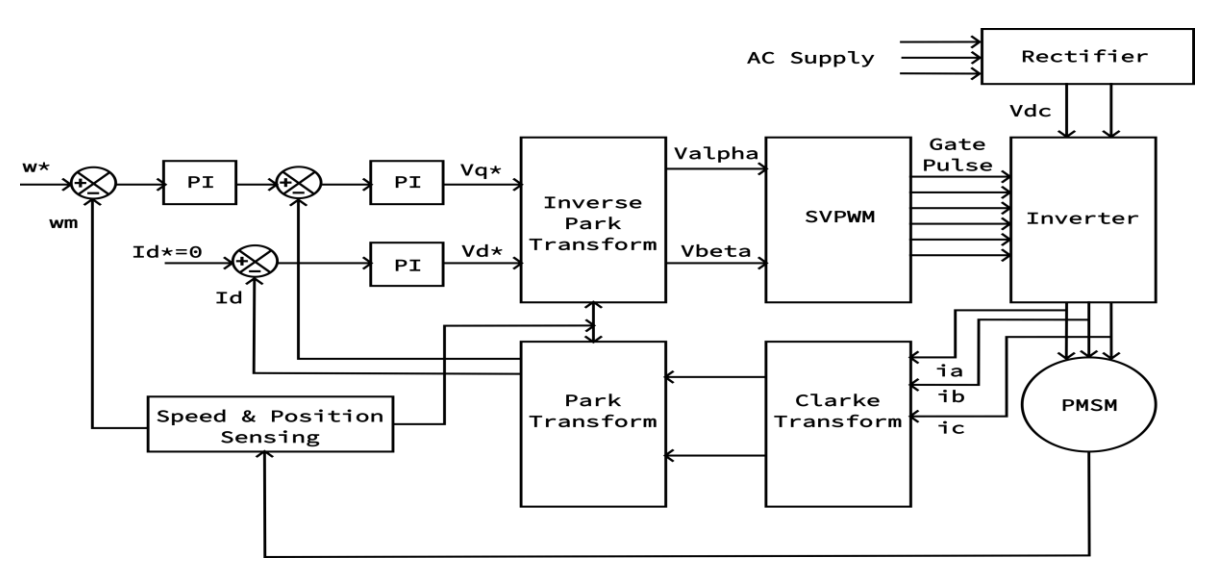


Figure 2. Field-oriented control (FOC) architecture.

The FOC architecture is shown in Figure 2. The Clarke and Park transformations are used to convert the three-phase stator currents into the d-q reference frame. The current controllers regulate the i_d and i_q currents, ensuring that the flux and torque-producing components are accurately controlled. Decoupling compensation is applied to address the cross-coupling effects between the d- and q-axes voltages. The inverse transformations convert the d-q voltages back to three-phase voltages for the pulse width modulation (PWM) generation, which ultimately drives the motor.

In this context, different PI controllers are used for the multiloop control action as follows:

i. Currents control loops

The current control loop involves two PI controllers to regulate the d-axis and q-axis currents: d-axis e-axis PI controller maintains the flux-producing current e-axis e-axis e-axis expressed as:

$$V_d^* = K_{PC_d} \left(i_d^* - i_d \right) + K_{IC_d} \int \left(i_d^* - i_d \right) . dt - \omega_e L_q i_q$$
 (1)

q-axis current control: The *q-axis* PI controller controls the torque-producing current i_q . The control law for the *q-axis* can be written as:

$$V_{q}^{*} = K_{PC_{q}} \left(i_{q}^{*} - i_{q} \right) + K_{IC_{q}} \int \left(i_{q}^{*} - i_{q} \right) . dt + \omega_{e} \left(L_{d} i_{d} + \lambda_{f} \right)$$
(2)

The outputs of these PI controllers, V_d^* and V_q^* , are the voltage references for the motor.

ii. Speed control loop

The speed control loop involves another PI controller that regulates the motor speed by providing the reference *q*-axis current based on the speed error.

The speed error is defined as:

$$e_{\omega} = \omega^* - \omega \tag{3}$$

where ω^* is the reference speed and ω is the actual speed.

The control law for the speed PI controller is given by:

$$i_q^* = K_{P\omega} e_\omega + K_{I\omega} \int e_\omega . dt \tag{4}$$

where $K_{p\omega}$, and $K_{l\omega}$ are the proportional, and integral gains for the speed PI controller, respectively.

This ensures that the motor operates at the desired speed by adjusting the torque.

iii. Analytical expressions of PI controller gains for current and speed control loops

The d-q axes current to input voltage ratios of PMSM are provided as,

$$\begin{cases}
\frac{i_d(s)}{u_d(s)} = \frac{\frac{1}{R_s}}{\frac{L_d}{R_s} s + 1} \\
\frac{i_q(s)}{u_q(s)} = \frac{\frac{1}{R_s}}{\frac{L_d}{R_s} s + 1}
\end{cases}$$
(5)

The series form of PI controller in term of its two coefficients (K₁, K₂) are mathematically expressed as,

$$PI(s) = K_1 + \frac{K_1 \cdot K_2}{s} \tag{6}$$

This is equivalent to parallel form of PI controller form i.e. K_{PC}+(K_{IC}/s). Thus,

$$\begin{cases}
K_{PC} = K_1 \\
K_{IC} = K_1.K_2 = K_{PC}.K_2
\end{cases}$$
(7)

The current control loop transfer functions for d-q axis currents are formed using (5)-(7) and which are given by,

$$\begin{cases}
\frac{i_{d}(s)}{i_{d}^{*}(s)} = \frac{\left(K_{PC_{-d}} + \frac{K_{IC_{-d}}}{S}\right) \frac{\frac{1}{R_{s}}}{\frac{L_{d}}{R_{s}} s + 1}}{1 + \left(K_{PC_{-d}} + \frac{K_{IC_{-d}}}{S}\right) \frac{\frac{1}{R_{s}}}{\frac{L_{d}}{S} s + 1}} = \frac{\left(K_{1_{-d}} + \frac{K_{1_{-d}}K_{2_{-d}}}{S}\right) \frac{\frac{1}{R_{s}}}{\frac{L_{d}}{R_{s}} s + 1}}{1 + \left(K_{1_{-d}} + \frac{K_{1_{-d}}K_{2_{-d}}}{S}\right) \frac{\frac{1}{R_{s}}}{\frac{L_{d}}{R_{s}} s + 1}}
\end{cases}$$

$$\frac{i_{q}(s)}{i_{q}^{*}(s)} = \frac{\left(K_{PC_{-q}} + \frac{K_{IC_{-q}}}{S}\right) \frac{\frac{1}{R_{s}}}{\frac{L_{q}}{R_{s}} s + 1}}{1 + \left(K_{1_{-q}} + \frac{K_{1_{-q}}K_{2_{-q}}}{S}\right) \frac{\frac{1}{R_{s}}}{\frac{L_{q}}{R_{s}} s + 1}}$$

$$1 + \left(K_{PC_{-q}} + \frac{K_{IC_{-q}}}{S}\right) \frac{\frac{1}{R_{s}}}{\frac{L_{q}}{R_{s}} s + 1}$$

$$1 + \left(K_{1_{-q}} + \frac{K_{1_{-q}}K_{2_{-q}}}{S}\right) \frac{\frac{1}{R_{s}}}{\frac{L_{q}}{R_{s}} s + 1}$$

$$1 + \left(K_{1_{-q}} + \frac{K_{1_{-q}}K_{2_{-q}}}{S}\right) \frac{\frac{1}{R_{s}}}{\frac{L_{q}}{R_{s}} s + 1}$$

The transfer functions in (8) can be simplified as,

$$\begin{cases}
\frac{i_{d}(s)}{i_{d}^{*}(s)} = \frac{\left(1 + \frac{S}{K_{2_{d}}}\right)}{\left(\frac{L_{d}}{K_{1_{d}}K_{2_{d}}}\right)s^{2} + \left(\frac{R_{s}}{K_{1_{d}}K_{2_{d}}} + \frac{1}{K_{2_{d}}}\right)s + 1} \\
\frac{i_{q}(s)}{i_{q}^{*}(s)} = \frac{\left(1 + \frac{S}{K_{2_{q}}}\right)}{\left(\frac{L_{q}}{K_{1_{q}}K_{2_{q}}}\right)s^{2} + \left(\frac{R_{s}}{K_{1_{q}}K_{2_{q}}} + \frac{1}{K_{2_{q}}}\right)s + 1}
\end{cases} \tag{9}$$

The polynomial in the denominator of (9) can be written as,

$$\begin{cases}
\left(\frac{L_d}{K_{1_{-d}}K_{2_{-d}}}\right)s^2 + \left(\frac{R_s}{K_{1_{-d}}K_{2_{-d}}} + \frac{1}{K_{2_{-d}}}\right)s + 1 = (1 + Es)(1 + Fs) \\
\left(\frac{L_q}{K_{1_{-q}}K_{2_{-q}}}\right)s^2 + \left(\frac{R_s}{K_{1_{-q}}K_{2_{-q}}} + \frac{1}{K_{2_{-q}}}\right)s + 1 = (1 + Gs)(1 + Hs)
\end{cases}$$
(10)

By comparing right-hand side terms with the left-hand side terms in (10), the following equations are obtained as,

$$\begin{cases}
\left(\frac{L_d}{K_{1_{-d}}K_{2_{-d}}}\right) = EF; \left(\frac{R_s}{K_{1_{-d}}K_{2_{-d}}} + \frac{1}{K_{2_{-d}}}\right) = E + F \\
\left(\frac{L_q}{K_{1_{-q}}K_{2_{-q}}}\right) = GH; \left(\frac{R_s}{K_{1_{-q}}K_{2_{-q}}} + \frac{1}{K_{2_{-q}}}\right) = G + H
\end{cases}$$
(11)

The solutions of (11) are obtained as,

$$\begin{cases}
\frac{R_s}{K_{1_d}K_{2_d}} = E; \frac{1}{K_{2_d}} = F \\
\frac{R_s}{K_{1_q}K_{2_q}} = G; \frac{1}{K_{2_q}} = H
\end{cases}$$
(12)

By putting (12) into (10) and (9), the (9) is expressed as,

$$\begin{cases}
\frac{i_{d}(s)}{i_{d}^{*}(s)} = \frac{\left(1 + \frac{S}{K_{2_{d}}}\right)}{\left(1 + \frac{R_{s}}{K_{1_{d}}K_{2_{d}}}S\right)\left(1 + \frac{S}{K_{2_{d}}}\right)} \\
\frac{i_{q}(s)}{i_{q}^{*}(s)} = \frac{\left(1 + \frac{S}{K_{2_{q}}}\right)}{\left(1 + \frac{R_{s}}{K_{1_{q}}K_{2_{q}}}S\right)\left(1 + \frac{S}{K_{2_{q}}}\right)}
\end{cases} (13)$$

The gains of series form of PI controller for d-q current control loop are derived from (13) as,

$$\begin{cases} K_{2_{-d}} = \frac{R_s}{L_d}; K_{1_{-d}} = L_d. (Bandwidth) \\ K_{2_{-q}} = \frac{R_s}{L_q}; K_{1_{-q}} = L_q. (Bandwidth) \end{cases}$$
(14)

In (14), the unit of bandwidth is taken as radian per sec (rad/sec).

From (7) and (14), the proportional and integral gains of parallel configuration of PI controller for d-q current control loop are obtained as,

$$\begin{cases} K_{PC_d} = K_{2_d} = L_d. (Bandwidth); K_{IC_d} = K_{1_d}.K_{2_d} = R_s. (Bandwidth) \\ K_{PC_q} = K_{2_q} = L_q. (Bandwidth); K_{IC_q} = K_{1_q}.K_{2_q} = R_s. (Bandwidth) \end{cases}$$
(15)

The desired bandwidth of the current control loop is 500 Hz (3141.6 rad/sec), which is (1/10) th [18] of the switching frequency (5 kHz).

The speed controller's bandwidth is considered as (1/20) th [18] of the bandwidth of current controller, which is taken as 25 Hz (157.08 rad/sec).

The proportional and integral gains of outer speed controller are designed using the expressions as,

$$K_{P\omega} = L_q.(Bandwidth/20); K_{I\omega} = R_s.(Bandwidth/20)$$
(16)

3 Conventional LQR-SFC based control logic for PMSM

The linear quadratic regulator (LQR) based state feedback control (SFC) is a more recent and sophisticated approach for speed control of PMSM [19]. This method involves designing a state feedback controller that aims to minimize a quadratic cost function. By doing so, it ensures optimal performance in terms of multiple control objectives, such as minimizing the error between the desired and actual speeds, reducing energy consumption, and improving overall system stability. The machine and control models are discussed as follows:

3.1 Mathematical model of PMSM

The PMSM is widely recognized for its efficiency and reliability in various industrial applications. To accurately model and control a PMSM, it is essential to transform the three-phase variables from the stator reference frame to a two-phase system in the rotor reference frame, commonly referred to as the d-q transformation [15]. This transformation simplifies the analysis and control of PMSM by aligning the rotor flux axis with the d-axis of the machine. One of the key assumptions in this modelling approach is that the inductance of the motor is independent of the rotor position, which simplifies the mathematical representation. The model can be written in state-space form as follows:

$$\frac{di_q}{dt} = \frac{v_q}{L_q} - \frac{R_s}{L_q} i_q - \omega_r \frac{L_d}{L_q} i_d - \omega_r \frac{\lambda_{af}}{L_q}$$
(17)

$$\frac{di_d}{dt} = \frac{v_d}{L_d} - \frac{R_s}{L_d} i_d + \omega_r \frac{L_q}{L_d} i_q \tag{18}$$

$$\frac{d\omega_r}{dt} = \frac{K_t}{J} i_q - \frac{B}{J} \omega_r - \frac{P}{J} T_L \tag{19}$$

where:

 $[i_a; i_d; \omega_r]$ are the states of the system.

 $[v_a; v_d]^T$ are the inputs.

 $d = -\frac{P}{J}T_L$ represents the load torque appearing on the motor, considered as an external disturbance.

 v_a and v_d are the q-axis and d-axis voltages, respectively.

 $R_{\rm s}$ is the stator resistance.

 i_a and i_d are the q-axis and d-axis currents, respectively.

 L_a and L_d are the q-axis and d-axis inductances, respectively.

 ω_r is the electrical angular velocity of the rotor.

 λ_{af} is the permanent magnet flux linkage.

 K_t is the torque constant.

J is the moment of inertia of the rotor.

B is the viscous friction coefficient.

 T_I is the load torque.

P is the number of pole pairs of the motor.

This state-space representation is crucial for the design and analysis of control systems for PMSM. By utilizing this form, one can apply various control strategies, such as state feedback control or observer-based control, to achieve desired performance characteristics.

3.2 Linearized model of PMSM

The model is linearized using Jacobian Linearization around an operating point $[i_{q0}, i_{d0}, \omega_{r0}]$ and this is given by:

$$\dot{x} = \begin{bmatrix}
-\frac{R_s}{L_q} & -\omega_{ro} \frac{L_d}{L_q} & -\frac{\lambda_f + L_d i_{do}}{L_q} \\
\omega_{ro} \frac{L_q}{L_d} & -\frac{R_s}{L_d} & \frac{L_q}{L_d} i_{qo} \\
\frac{K_t}{J} & 0 & -\frac{B}{J}
\end{bmatrix} x + \begin{bmatrix}
\frac{1}{L_q} & 0 \\
0 & \frac{1}{L_d} \\
0 & 0
\end{bmatrix} u + \begin{bmatrix}
0 \\
0 \\
1
\end{bmatrix} d$$
(20)

where:

 \dot{x} represents the state derivative vector of the PMSM.

x denotes the state vector, consisting of currents id; iq and angular velocity !.

u is the input vector, which typically includes the applied voltages in d- and q-axis.

d represents the disturbance vector, commonly associated with variations in load torque.

 R_s , L_d , L_q , λ_f J, and B are motor-specific constants: stator resistance, d-q axis inductances, permanent

magnet flux linkage, rotor inertia, and damping coefficient, respectively.

 $i_{do} = i_d^* = 0$ since the control scheme demands a constant $\delta = 90^\circ$, resulting in $i_d = 0$.

 $\omega_{ro} = \omega_r^*$ is the reference speed, which is a constant value for the regulator system.

 $i_{qo} = i_q^*$ changes with the load torque.

3.3 Linear quadratic regulator-based state feedback control of PMSM drive

The design of a linear quadratic regulator (LQR) based SFC [19-21] for controlling the PMSM revolves around the formulation of a state feedback control strategy that minimizes a cost function representing a trade-off between system performance and control effort. This section provides a discussion on the formulation and solution of the LQR control problem applied to PMSM's speed control.

The core concept of the LQR design defines a cost function J, which is to be minimized:

$$J = \int_{0}^{\infty} \left(x^{T} Q x + u^{T} R u \right) dt \tag{21}$$

where:

Q is a symmetric positive semi-definite matrix,

R is a symmetric positive definite matrix.

x is the state vector,

u is the input vector,

These matrices weight the relative importance of states and control efforts in the cost function. The choice of Q and R significantly affects the controller's performance and robustness.

Given the linearized model obtained by Jacobian linearization, the state-space representation can be expressed as:

$$\dot{x} = Ax + B_u u + B_d d \tag{22}$$

The output equation is presented as,

$$y = Cx \tag{23}$$

where the matrices A, B_u , B_d , and C are defined as:

$$A = \begin{bmatrix} -\frac{R_s}{L} & -\omega_o & -\frac{\lambda_f + LI_{do}}{L} \\ \omega_o & -\frac{R_s}{L} & I_{qo} \\ \frac{K_t}{J} & 0 & -\frac{B}{J} \end{bmatrix}$$
(24)

$$B_{u} = \begin{bmatrix} \frac{1}{L} & 0\\ 0 & \frac{1}{L}\\ 0 & 0 \end{bmatrix}$$
 (25)

$$B_d = \begin{bmatrix} 0 \\ 0 \\ 1 \end{bmatrix} \tag{26}$$

$$C = \begin{bmatrix} 0 & 0 & 1 \end{bmatrix} \tag{27}$$

Here, the state vector $x = \begin{bmatrix} i_q & i_d & \omega \end{bmatrix}^T$ represents the q-axis current, d-axis current, and angular velocity, respectively. The input vector $u = \begin{bmatrix} v_q & v_d \end{bmatrix}^T$ corresponds to the q-axis and d-axis voltage inputs, and d represents any disturbances. The vectors $\begin{bmatrix} i_{qo} & i_{d0} & \omega_o \end{bmatrix}^T$ indicate the steady-state operating point of the system.

The linear SFC, obtained via the LQR approach, is designed to track desired outputs by compensating the deviation between the reference and actual states. The control law is given by:

$$u = -K\left(x^* - x\right) \tag{28}$$

where x^* are the reference states, x are the actual states, and K is the state feedback gain matrix. This conventional SFC is designed using state errors to ensure the system tracks the desired trajectory effectively.

Here K is calculated by solving the Continuous Algebraic Riccati equation (CARE):

$$A^{T}P + PA - PBR^{-1}B^{T}P + Q = 0 (29)$$

P is a symmetric positive definite matrix, and the optimal gain matrix K is then given by:

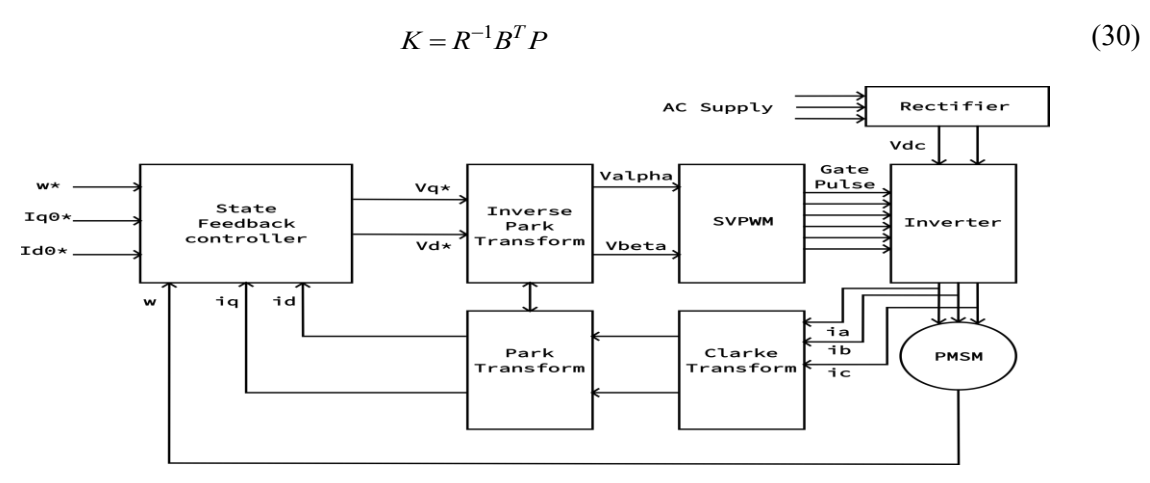


Figure 3. Architecture of SFC.

4 Integral action based LQR-SFC logics

The different integrals action based LQR-SFC logics are presented as follows:

4.1 LQR-SFC with PI control (LQE-SFC-PI control)

The control logic is shown in Figure 4. Here, the PI controller decides the required torque and q-axis current for the LQR-SFC model. This will provide additional control action along with the LQR-SFC model described in section 3.3.

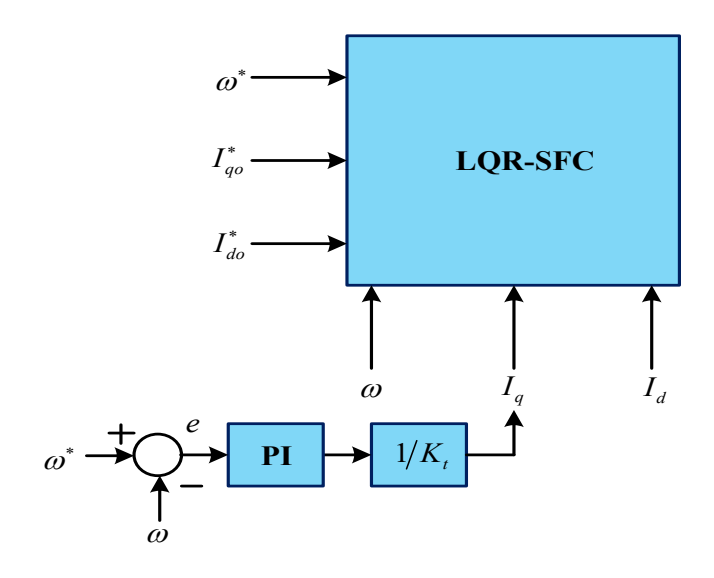


Figure 4. LQR- SFC-PI control.

4.2 LQR-SFC with integral speed error control (LQE-SFC-ISE control)

In the logic, the integration of speed error (ISE) is used as the additional input in the LQR-SFC model to obtain optimized speed response. The control scheme is given in Figure 5.

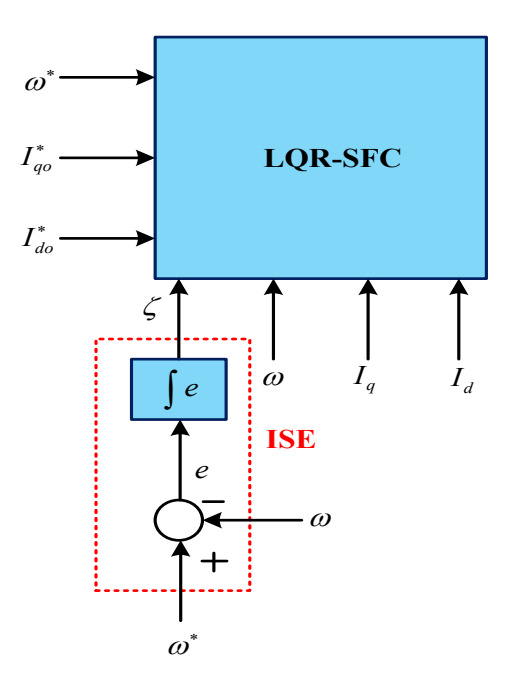


Figure 5. LQR- SFC-ISE control.

The controller design [9] is as follows:

$$u = -K_x \left(x^* - x \right) + K_i \zeta \tag{31}$$

where ζ is an integral state defined by the equation:

$$\dot{\zeta} = \left(\omega^* - \omega\right) \tag{32}$$

Here, ω^* represents the desired angular velocity and ω the actual angular velocity. K_x is the state feedback gain matrix, and K_i is the integral gain matrix, both of appropriate dimensions. This ISE is achieved by augmenting the state equation to include integral action, which ensures zero steady-state error by integrating the difference between the desired and actual speed outputs.

To include integral action in the state feedback control strategy, the state-space model is modified by combining both equations involving states x and ζ . This results in the following augmented state-space model:

$$\begin{bmatrix} \dot{x}(t) \\ \dot{\zeta}(t) \end{bmatrix} = \begin{bmatrix} A & 0 \\ -C & 0 \end{bmatrix} \begin{bmatrix} x(t) \\ \zeta(t) \end{bmatrix} + \begin{bmatrix} B \\ 0 \end{bmatrix} u(t) + \begin{bmatrix} B_d \\ 0 \end{bmatrix} d(t) + \begin{bmatrix} 0 \\ 1 \end{bmatrix} \omega^*(t)$$
(33)

where,

- x(t) is a state vector representing the system's current state.
- $\zeta(t)$ is integral of the error, integrating the difference between the desired and actual outputs over time.
- u(t) is a control input, representing the action taken by the controller to drive the system.
- d(t) is an external disturbance, accounting for any external factors affecting the system.
- $\omega^*(t)$ is time-varying desired angular velocity, influencing the integral part of the state vector to track the desired trajectory.

This model effectively extends the original state dynamics by incorporating a feedback mechanism that integrates the speed error over time, aiming to eliminate steady-state errors and improve overall control performance.

5 Studies, results, and observations

The different studies, results, and observations on comparative performances of PMSM drive with different control techniques are discussed. The machine parameters are specified in Table 2. The simulations of different models are done to find out the performance parameters such as overshoot, rise time, settling time, and steady-state error, with visual representations of the system's dynamic response at the starting moment. The case studies and responses are obtained using Matlab-Simulink software.

F					
Parameters	Values				
No of pole pairs	4				
L_q	3.2 mH				
L_d	1.7 mH				
R_S	$22.2~\mathrm{m}\Omega$				
λ_f	39.6 mWb				
J	$0.008~\mathrm{kg.m^2}$				
R_{\cdots}	0.001 Nms				

Table 2. Machine parameters.

Table 3. PI controller gains.

Proportional gain (K _P)	Integral Gain (K _I)
0.2	5

The study focuses on the speed control of a PMSM using traditional LQR-based state feedback control along with PI controller for regulating q-axis current (LQR-SFC-PI), and LQR-SFC with integral of speed error (LQR-SFC-ISE). The modeled PMSM drive systems in MATLAB-SIMULINK mainly conduct a detailed study and comparison of these two control strategies.

The weight matrices of are taken in the two different control models are taken as,

For the LQR control with PI controller, the weight matrices $Q \ge 0$ and $R \ge 0$ are taken as:

$$Q = \begin{bmatrix} 30 & 0 & 0 \\ 0 & 5 & 0 \\ 0 & 0 & 50 \end{bmatrix}; R = \begin{bmatrix} 1 & 0 \\ 0 & 1 \end{bmatrix}$$

The gains of PI controller are given in Table 3, which are obtained from autotuning of PI controller in SIMULINK software.

For the LQR-SFC-ISE control, the weight matrices $Q \ge 0$ and $R \ge 0$ are used as:

$$Q = \begin{bmatrix} 1 & 0 & 0 & 0 \\ 0 & 1 & 0 & 0 \\ 0 & 0 & 2 & 0 \\ 0 & 0 & 0 & 20 \end{bmatrix}; R = \begin{bmatrix} 1 & 0 \\ 0 & 1 \end{bmatrix}$$

Both control models are tested and the following case studies are presented as follows:

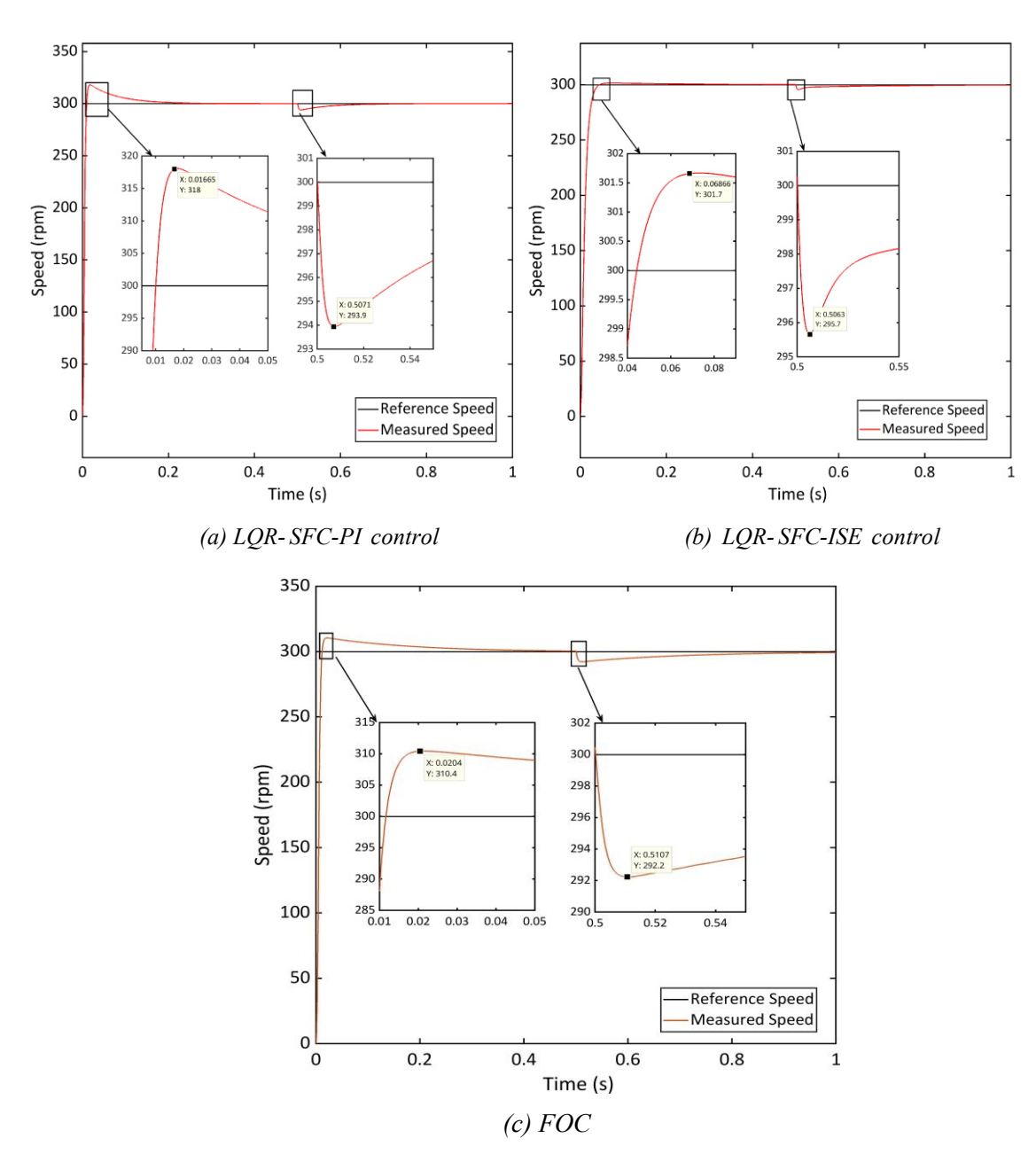


Figure 6. Speed response of PMSM for different control methods.

5.1 Performance at low rotational speed

In the test scenario, the motor runs with a reference speed of 300 rpm. At time (t) = 0.5 seconds, a load of 2 Nm is applied to the motor. By observing the system's response to this load disturbance, the performance of each control method is evaluated in terms of steady state and transient effects. The dynamic responses of PMSM using various control models at the test condition (rotational speed of 300 rpm) are given in Figure 6 and Figure 7. Figure 6 shows the speed responses of the motor for different control models. By comparing the speed responses, the overshoot or undershoot and settling time is significantly reduced in case of LQR-SFC-ISE than that of LQR-SFC-PI and FOC techniques. The corresponding d-q axes currents and torque responses for the different control methods are presented in Figure 7. The comparative performance parameter values in Table 4 highlight the strengths and weaknesses of each control strategy in the application.

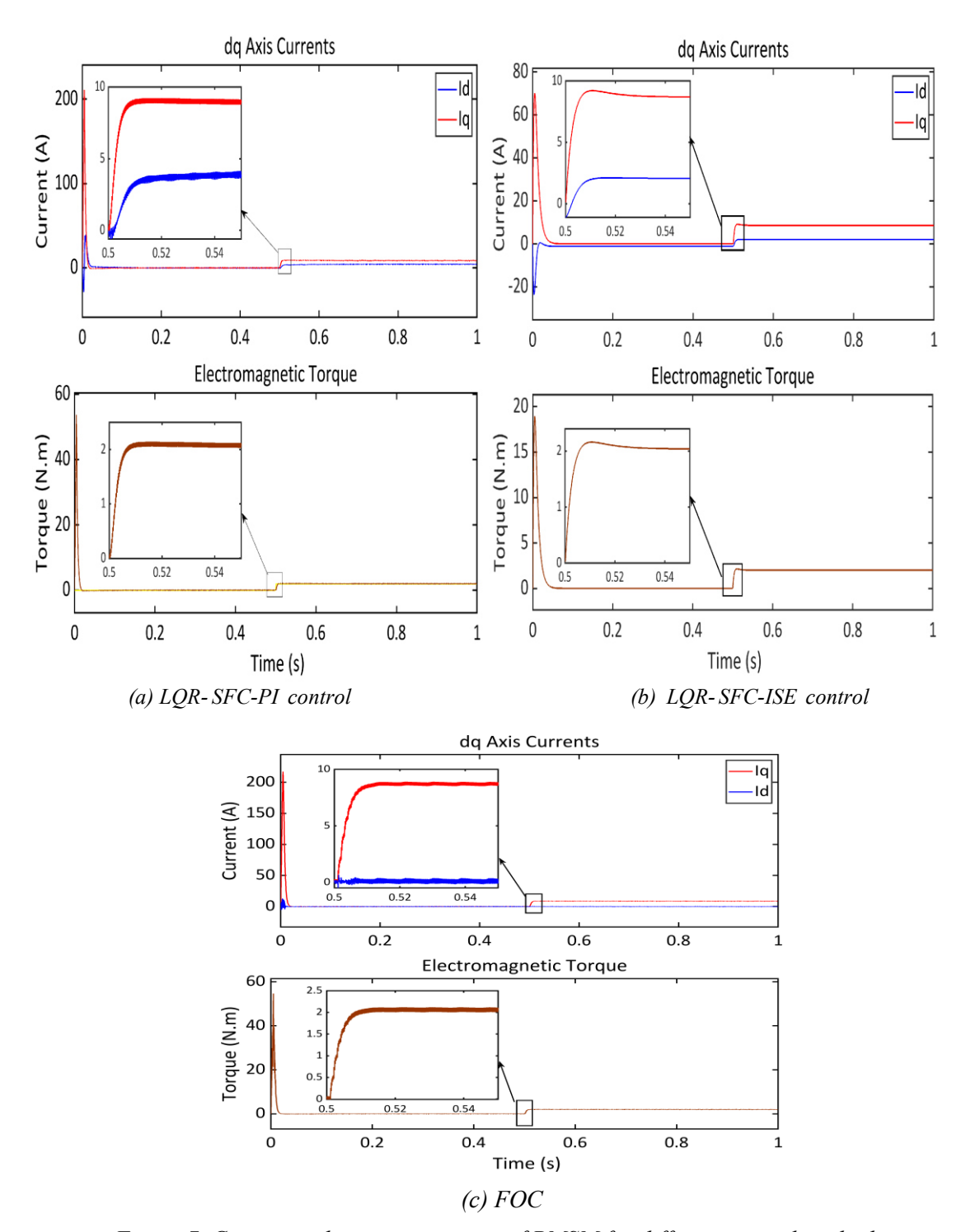


Figure 7. Current and torque responses of PMSM for different control methods.

The settling times for the different speed control methods are displayed in Figure 8, which are listed in Table 4. For the settling time, a 0.5% steady-state error criterion is used.

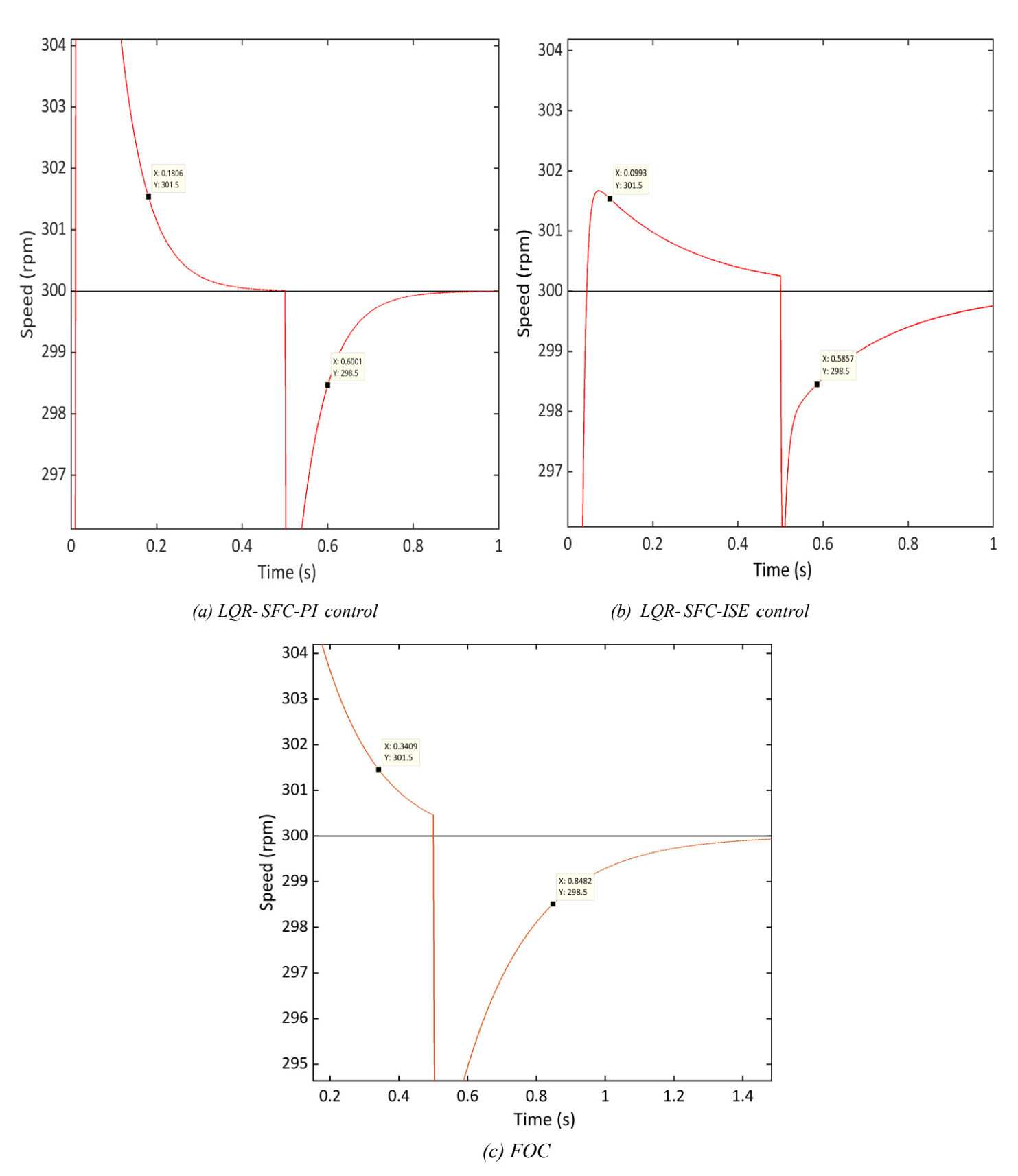


Figure 8. Settling time of speed responses of PMSM for different control methods.

Control	Parameters of speed response				Parameters of torque response			
Method	Rise time (s)	Settling time (s)	Peak overshoot (%)	Steady state error (%)	Rise time (s)	Settling time (s)	Peak undershoot (%)	Steady state error (%)
FOC [15]	0.014	0.341	346	0.2	0.011	0.848	-2.6	-0.2
LQR-SFC- PI	0.0083	0.181	6	0	0.007	0.1	-2	0
LQR-SFC- ISE	0.040	0.099	0.566	0.1	0.005	0.086	-1.43	-0.1

Table 4. Comparative performance at low speed (300 rpm) with step change in torque (t=0.5 s).

5.2 Performance at high rotational speed

In the test scenario, the motor is controlled for a reference speed of 1500 rpm. At time (t) = 0.5 seconds, a load of 2 Nm is applied to the motor. The comparative dynamic speed responses of two LQR-SFC models (LQR-SFC-PI and LQR-SFC-ISE) are presented in Figure 9 to illustrate the comparative effects of the two integral control actions on the conventional LQR-SFC based PMSM drive. Figure 9(a) shows that the motor fails to attain the desired speed for the LQR-SFC-PI model from the starting moment, whereas LQR-SFC-ISE method based PMSM drive converges to the reference speed. This indicates robust dynamic performance of LQR-SFC-ISE technique in the drive application.

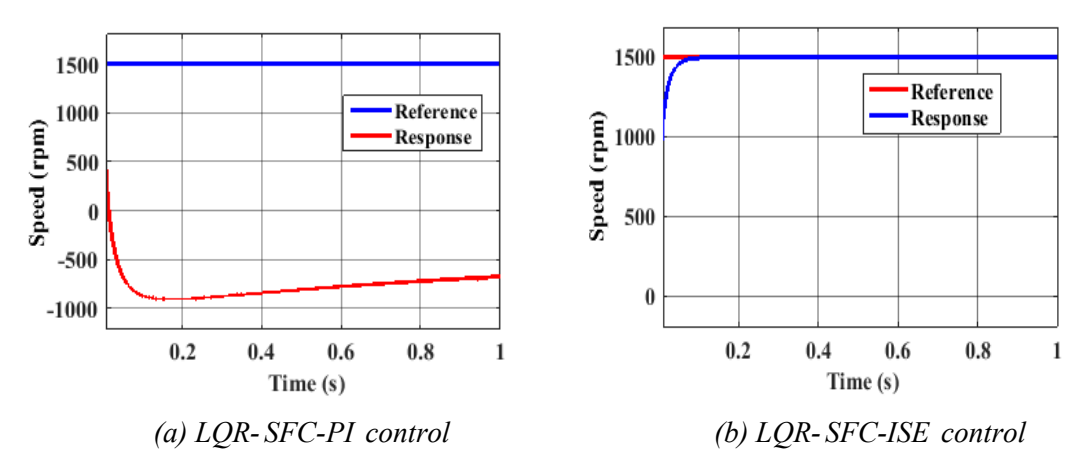


Figure 9. Speed responses of PMSM at 1500 rpm.

The data on comparative performances of the two integral controls based LQR-SFC model are listed in Table 5. Figure 9(a) reveals that the speed response is not settled to the reference speed. Therefore, the performance parameter values for LQR-SFC-PI case are missing in Table 5.

Control Method	Parameters of speed response				Parameters of torque response			
	Rise time (s)	Settling time (s)	Peak overshoot (%)	Steady state error (%)	Rise time (s)	Settling time (s)	Peak undershoot (%)	Steady state error (%)
LQR-SFC- PI	-	-	-	-	-	-	-	-
LQR-SFC- ISE	0.06	0.099	1	0.2	0.044	0.281	-1.46	-0.2

Table 5. Comparative performance at high speed (1500 rpm) with step change in torque (t=0.5 s).

5.3 Performance under load torque variations

The load torque variation effects for the different integral control actions with LQR-SFC models are investigated, and corresponding results are presented in Figure 10 and Figure 11. Here, load torque changes from 3 N-m to 2 N-m at t=0.4 s and from 2 N-m to 3 N-m at t=0.7 s. The speed reference is set at 1500 rpm. The load torque variations cause the unstable operation in the case of LQR-SFC-PI, which is shown in Figure 10. But the stable operation of the LQR-SFC-ISE-based PMSM drive occurs under the load variations, which is presented in Figure 11.

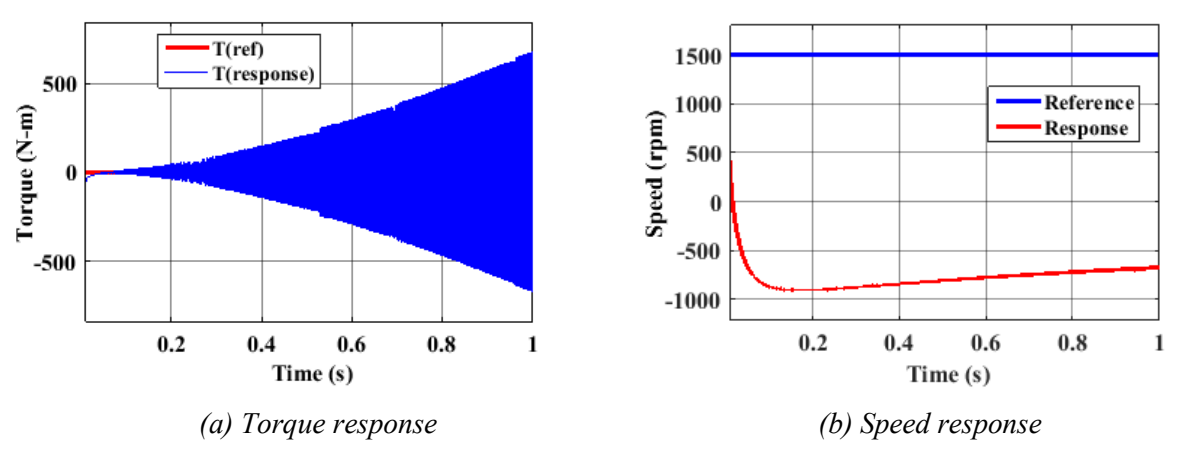


Figure 10. Speed and torque responses of PMSM at load torque variations under LQR-SFC-PI method.

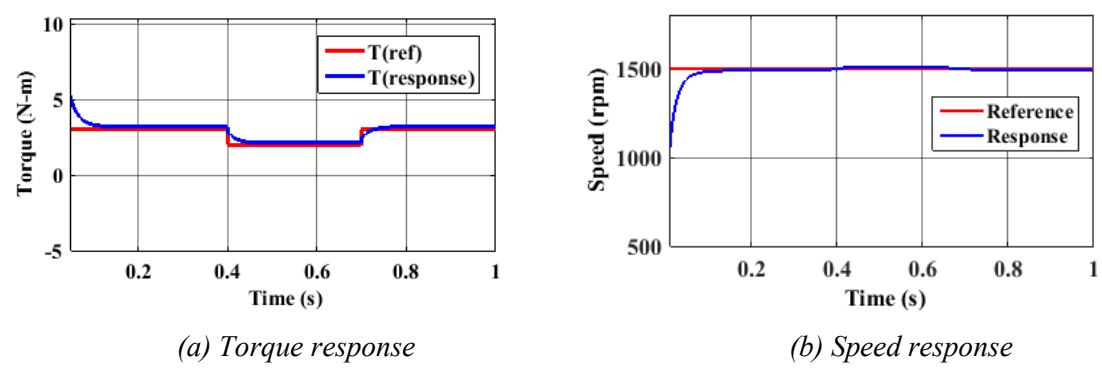


Figure 11. Speed and torque responses of PMSM at load torque variations under LQR-SFC-ISE method.

5.4 Observations

The following observations are listed from different studies:

- i. From the results, it is evident that, the LQR-SFC-ISE control provides the best overall performance, demonstrating minimal overshoot and undershoot from the motor's reference operating point than the LQR-SFC-PI control (Table 4).
- ii. The settling time is less in case of LQR-SFC-ISE control than LQR-SFC-PI control (Table 4).
- iii. The rise time is slightly more in case of LQR-SFC-ISE control than LQR-SFC-PI control (Table 4).
- iv. The steady state error slightly more in case of LQR-SFC-ISE control than LQR-SFC-PI control, but both are acceptable (Table 4).
- v. In case of high-speed reference, the LQR-SFC-PI control fails to attain the reference speed (Figure 9(a)), which indicates the speed diverges from the reference speed in the starting point. On the other hand, dynamic speed response under LQR-SFC-ISE control is satisfactory, and robust and it finally reaches to the required high-speed speed (Figure 9(b)).

6 Conclusion

This paper provides the comparative performances of two types (LQR-SFC-PI and LQR-SFC-ISE) integral control action-based state feedback controller. Here, the desired steady state and transient performances are investigated under different speed conditions. The steady state error of the speed response is almost similar with the both integral actions. Bur the transient response of LQR-SFC-ISE is found different pattern from that of LQR-SFC-PI. The LQR-SFC-ISE reduces the peak overshoot or undershoot and settling time, whereas LQR-SFC-PI reduces rise time. Here, the dynamic performances of both models are also investigated under high-speed reference from the zero speed at the starting point. Here, it is noticed that the speed response is rising toward the reference speed in case of the LQR-SFC-ISE model, whereas the LQR-SFC-PI model is not able to catch the reference speed and diverges significantly just after the starting point.

Therefore, this study reveals the following observations:

- i. Different dynamic performance for two integral actions along with the standard LQR-SFC method of the PMSM drive system is noticed.
- ii. The dynamic performance of the LQR-SFC-PI control technique at the starting moment is different from the low-speed reference to the high-speed reference for the same gains of the PI controller. The speed response converges for low-speed values, whereas the response diverges for the high-speed value.
- iii. The dynamic performance of the LQR-SFC-ISE method is robust, which behaves almost in a similar manner for low-speed and high-speed references for the same parameters of the matrices.

References

- [1] R. Krishnan, Permanent Magnet Synchronous and Brushless DC Motor Drives. CRC Press, 2010.
- [2] S. Singh, S. N. Singh, and A. N. Tiwari, "PMSM Drives and its Application: An Overview" *Recent Advances in Electrical & Electronic Engineering*, vol. 16, no. 1, pp. 4-16, Sept. 2023.
- [3] K. Thangarajan, and A. Soundarrajan. "Performance comparison of permanent magnet synchronous motor (PMSM) drive with delay compensated predictive controllers". *Microprocessors and Microsystems*, vol. 75, pp. 103081, Jun. 2020.
- [4] R.E.K. Meesala, S. Athikkal, P. Pradhan, S. Prasad, and A. Prasad. "Modified Direct Torque Control of PMSM Drive for Electric Vehicle Application". *In Proceedings of the IEEE Madras Section Conf. (MASCON)*, Aug. 2021; pp. 1-5.
- [5] J. Hong, X. Lin, J. Zhang, Y. Xu, B. Yan, and X. Li. "A state feedback control with compensation for permanent magnet synchronous machine drives". *ISA Trans.*, vol. 150, pp. 232-242, Jul. 2024.
- [6] Z. Feng, S. Baig, S. Ebrahimi, J. Jatskevich. "A Novel State-Feedback Controller for Permanent Magnet Synchronous Machines". In: 2023 International Conference on Modeling, Simulation & Intelligent Computing (MoSICom), Dec. 2023, pp. 191-196.
- [7] C.O. Omeje, A.O.Salau, and C.U. Eya. "Dynamics analysis of permanent magnet synchronous motor speed control with enhanced state feedback controller using a linear quadratic regulator". *Heliyon*, vol. 10, no. 4. pp. e26018, Feb. 2024.
- [8] A. A. Apte, V. A. Joshi, R. A. Walambe, and A. A. Godbole, "Speed control of PMSM using disturbance observer," *IFAC-Papers OnLine*, vol. 49, no. 1, pp. 308-313, 2016.
- [9] A. Apte, V. A. Joshi, H. Mehta, and R. Walambe, "Disturbance-observer-based sensorless control of PMSM using integral state feedback controller," *IEEE Trans. Power Electron.*, vol. 35, no. 6, pp. 6082-6090, Jun. 2020.
- [10] B. Zhang, and X. Tang. "High-performance state feedback controller for permanent magnet synchronous motor". *ISA Trans.*, vol. 118, pp. 144-158, Dec. 2021.
- [11] R. Szczepanski, T. Tarczewski, and L. M. Grzesiak, "Adaptive state feedback speed controller for PMSM based on artificial bee colony algorithm," Appl. Soft Comput., vol. 83, Oct. 2019, Art. no. 105644.
- [12] D.W. Novotny and T.A. Lipo. *Vector control and dynamics of AC drives*. Oxford University Press, 1996.
- [13] D.O. Neacsu. "Space vector modulation-An introduction". In: *IECON 2001: The 27th Annual Conf. of the IEEE Ind. Electron. Society (Cat. No. 37258), IEEE*, 2001, pp. 1583-1592.
- [14] X. Sun, L. Niu, and S. Yan. "MPC-PI cascade control method for heavy-haul train". In: 2019 IEEE Intelligent Transportation, Oct. 2019, pp. 2527-2532.
- [15] H. Ghanayem, M. Alathamneh, R.M. Nelms. "Three-phase PMSM vector control using decoupled flux and Speed Controller". *Energy Rep.*, vol. 9, pp. 645-652, 2023.
- [16] H. Ghanayem, M. Alathamneh, R.M. Nelms. "Adaptive PIR current controllers for torque ripple reduction of PMSM using decoupled speed and flux control". In: 2023 IEEE 14th Annual Ubiquitous Computing, Electronics & Mobile Communication Conference (UEMCON), Oct. 2023, pp. 440-444.
- [17] F. Amin, E. Sulaiman, and H.A. Soomro. "Field-oriented control principles for synchronous motor". *Int. J. of Applied Engineering Research*, vol. 8, no. 2, pp. 284-288, Mar. 2019.
- [18] D. Zhou, and F. Blaabjerg, "Bandwidth oriented proportional-integral controller design for back-to-back power converters in DFIG wind turbine system," *IET Renew. Power Gen.*, vol. 11, no. 7, pp. 941-951, Jun. 2017.
- [19] A. Shahzad, S. Munshi, and S. Azam. "Design and Implementation of a State-feedback Controller Using LQR Technique". In: *Computers, Materials & Continua*, vol. 73, no. 2, pp. 2897-2911, Jun. 2022.
- [20] M.I. Solihin, Wahyudi, A Legowo, and R. Akmeliawati. "Comparison of LQR and PSO-based state feedback controller for tracking control of a flexible link manipulator". In: 2010 2nd IEEE Int. Conf. on Inform. Management and Engineering, Apr. 2010, pp. 354-358.

[21] TV Tran, KH Kim, and JS Lai. " $H_2/H\infty$ Robust Observed-State Feedback Control Based on Slack LMI-LQR for LCL-Filtered Inverters". In: *IEEE Trans. on Ind. Electron.*, vol. 70, no. 5, pp. 4785 - 4798, Jul. 2022.